Conference Paper

Induction Motor Thermal Analysis Based on Lumped Parameter Thermal Network

Pedro Cabral and Amel Adouni

CISE | Electromechatronic Systems Research Centre, University of Beira Interior

Abstract

Many industry applications required the use of the induction motors. In such envirenement the electrical machines are facing of many stressed operating conditions. One of the critical creteria which decide the choice of the induction motor is the thermal behaviour under different mode operation. In this paper a study of the thermal behavior of an induction motor is presented. In order to predict the temperature in the different machine components, a model based on the lumped parameter thermal network has been developed. The geometry of the machine and the thermal properties of its various components are used to express the developed model. The joule and the iron losses are considering as the inputs. The proposed model is implemented and tested using MATLAB software. It is a simple model which could predict rapidly the different temperatures.

Keywords: Induction motor, Thermal analysis, Lumped parameters thermal network, Modeling, Heat sources

Corresponding Author:
Pedro Cabral
pedro_c_a96@hotmail.com

Received: 26 November 2019
Accepted: 13 May 2020
Published: 2 June 2020

Publishing services provided by Knowledge E

Selection and Peer-review under the responsibility of the ICEUBI2019 Conference Committee.

1. Introduction

The induction motor (IM) is one of the most widely used industrial machines. This choice is justified by its robustness, efficiency, reliability and low cost [1]. The IM recorded almost 64% of industrial electricity consumption [2]. So, it's extremely useful to study in detail the different behaviours of this equipment. These machines are usually operating in a stressed environment with sometimes small space available. Such operating conditions cause a heat concentration. Actually an increasing in the temperatures can lead to failures in the machine and a decreasing in the useful lifetime. That's why, the thermal behaviour of the IM is considering as a critical criteria based on it the IM is chosen. It becomes very important to predict the temperature behaviour in critical points of the IM. Such study could help to judge the control the IM from the thermal point of view [3].

The thermal study is mainly based on the description of the heat paths. Since, the electric machine is a relatively complex system, such description presents some difficulty. In the beginning, when the computing systems have been not yet developed, the first attempts to predict the thermal behaviour of the IM were based on empirical

formulas derived from experimental measurements [4]. Nowadays, it's possible to find several tools and methods at our disposal. In the literature, the thermal analysis can be studied based on two different types of approaches: analytical methods or numerical methods. Both approaches are based on the description of a physical phenomenon, such as heat conduction, heat transfer and heat convection, through a mathematical relations which are partial differential equations (PDE). For a simple thermal description, the solution of these equations can be obtained using analytical methods. The provided solution is an average of the temperature. The analytical method is simple and rapid but limited in terms of a temperature distribution. However, for more complex issues such as design issue, the thermal description needs to be solved by a numerical approach. The numerical analysis can be done using two types of methods: Computational Fluid Dynamics (CFD) or Fine Element Analysis (FEA) [5]. The main advantage of these methodologies is the fact that they can deal with a complex geometry [6]. However, they require a lot of time during the simulations process. In this paper, the analytical method is used. It is well known as, the Lumped Parameter Thermal Network (LPTN). The LPTN has been the subject of many works in the literature and it is used for the thermal analaysis of the IM working in the healthy and faulty mode operations [7-8]. The basic idea relies on an analogy between the electrical and thermal grids. The electrical machine is geometrically discretized into a local element, each one interconnected with its neighbour through thermal resistances. This method is very fast and could be implemented online. To apply this approach, the analytical model of the IM is in order to quantify the losses. The different losses presented the inputs of the LPTN model.

2. Induction Motor Modelling

In order to obtain the losses of the IM it is necessary to develop an analytical model that describes its electromagnetic and mechanical behaviours. This model is based on the equivalent scheme proposed by the IEEE. The development of a model in the abc framework presents some difficulty, the d-q0 transform was applied to simplify the modeling process. So, instead of a three-phase model, a two phases model is sufficient. This approach simplifies the calculations. The Park transformation will be used in order to obtain the two phase system model.

2.1. Electrical description

The stator voltages in the dq0 frame are expressed using the equations (1) and (2) [9].

$$V_{ds} = R_s.i_{ds} + \frac{d\Psi_{ds}}{dt} - \omega_e.\Psi_{qs} \tag{1}$$

$$V_{qs} = R_s.i_{qs} + \frac{d\Psi_{qs}}{dt} + \omega_e.\Psi_{ds} \tag{2}$$

Where R_s is the stator resistance. The i_{ds}, i_{qs} are the stator currents and ψ_{ds}, ψ_{qs} are the stator flux linkages.

The rotor voltages in the dq0 frame are expressed using the equations (3) and (4) [9]. The motor under study is a squirrel cage induction motor. Hence the rotor voltages are nulls.

$$V_{dr} = R_r.i_{dr} + \frac{d\Psi_{dr}}{dt} - (\omega_e - \omega_r).\Psi_{qr} \tag{3}$$

$$V_{qr} = R_r.i_{qr} + \frac{d\Psi_{qr}}{dt} + (\omega_e - \omega_r).\Psi_{dr} \tag{4}$$

Where i_{dr} and i_{qr} are the rotor currents and ψ_{dr}, ψ_{qr} are the rotor flux linkages

2.2. Magnetic model

From the magnetic model the stator and rotor flux linkages are defined based on the equations (5-8).

$$\Psi_{ds} = L_s.i_{ds} + L_m.i_{dr} \tag{5}$$

$$\Psi_{qs} = L_s.i_{qs} + L_m.i_{qr} \tag{6}$$

$$\Psi_{dr} = L_r.i_{dr} + L_m.i_{ds} \tag{7}$$

$$\Psi_{qr} = L_r.i_{qr} + L_m.i_{qs} \tag{8}$$

Where L_s, L_r are the stator and rotor linkage inductance. L_m is the mutual magnetizing inductance.

2.3. Mechanical model

In the mechanical model, we define the torque (T) and speed (ω). The speed is a function of the calculated torque, the rotor inertia (J) and the torque load (C_r).

$$T = \frac{pL_m}{L_r}(\Psi_{dr}i_{qs} - \Psi_{qr}i_{ds}) \tag{9}$$

$$\omega = \int \frac{T - C_r}{J} \tag{10}$$

Where p represents the number of pairs poles of the machine.

2.4. Losses

Despite the high efficiency of the asynchronous machine, a part of electrical energy is converted to useful mechanical energy. The rest of energy is dissipated in a form of heat. Most of the losses are due to the magnetic fields and currents [8]. The losses are classified mainly into: Joule losses, iron losses and mechanical losses. During the operation mode, the different losses which increase the heat affect the efficiency and performance of the IM. When they exceed the permitted thermal limit, may lead to decrease the lifetime [1].

2.4.1. Joule losses

Joule losses (P_J) presents the big part of the total losses. They depend of the stator and rotor currents. The rotor currents are almost nulls. Hence, the rotor joule losses are neglected. These losses are computed based on the Joule's law which states the relationship between the losses generated by a current flow through a conductor. The power dissipated by the conductor, in this case, by the windings, is proportional to the resistance of the conductors and to the square of the current. Actually, the winding resistance dependents of the temperature, so these losses are also influenced by the machine's thermal behaviour. In the present work, we will be considered as a constant. For three phase systems, these losses are computed using the equation (11).

$$P_J = R_a I_a^2 + R_b I_b^2 + R_c I_c^2 \tag{11}$$

Where R_a, R_b, R_c represent the resistances of the three phase windings and I_a, I_b and I_c the currents in each phase.

2.4.2. Iron losses

The iron losses (P_f), known also as core losses, are generated due to the variation of the magnetic field which occur in the ferromagnetic materials.

These losses are divided into hysteresis losses (static losses), eddy current losses (dynamic losses), and high-frequency losses (excess losses). The iron losses occur in the stator ferromagnetic core laminations and in the rotor. They result from the presence

of the magnetic flux, and are strongly dependent on the material magnetic properties, the supply voltage frequency, and the geometry of the machine. The iron losses mainly occur in the stator magnetic sections, because the frequency of the rotor flux is low, so the rotor losses are neglected [10]. The Iron losses are usually calculated using empirical models such as Steinmetz's model [11] but can also be calculated using mathematical models like Bertotti's formula. In this paper approximation formula was used. It gives a rudimentary value of core losses.

$$P_f = \frac{3.V_{RMS}^2}{R_{ferro}} \tag{12}$$

2.4.3. Mechanical losses

Mechanical losses occur due ventilation losses and bearing friction. The ventilation losses result from the friction between the rotor surface and the air in the air gap. Therefore, the higher the rotor speed, the greater is the friction and consequently the losses. Moreover, in ventilated motors, the energy required to move the fan is classified as ventilation losses. The bearing losses result from the friction in the contact areas, particularly in the rolling elements and raceways, between the rolling elements and the cage, and between other surfaces [12]. These losses are influenced by many factors such as, the machine rotational speed, the bearing type, the lubricant properties, temperature and other [design rotating machines]. At high rotational speeds ventilation losses are the predominant component. Friction and ventilation losses are usually determined experimentally, as in [13].The bearing losses (P_b) were calculated based on the SKF recommendations through the follow expression:

$$P_b = 0,5.\Omega.F.D_b.\mu \tag{13}$$

This expression is a funcontion of the, Ω which reprsent de angular frequency of the shaft, F that represents the bearing load, D_b, the bearing inner diameter and μ, the friction coefficient. This coeficiente can be obtained in the manufacter data and usually assumes a value between 0.001–0.05.

Regarding the ventilation losses, they result from the friction caused by the outer and the end surfaces of the rotor with the air. The calculation of these losses depends on certain parametres and is based in [12]. Respecting the friction of the outer surface with air, can be modultaed through the folow equation:

$$P_{W1} = \frac{1}{32} K.C_{M1}.\pi.\rho.\Omega^3.D_r^4.l_r \tag{14}$$

Where K is a roughness coefficient of the surface, C_{M1} a torque coefficient, ρ the density of air, Ω the angular velocity of the rotor, D_r is the rotor diameter and l_r the rotor length. The torque coefficient is a function of the Couette Reynolds (Co) number.

$$Co = \frac{\rho \Omega D_r \delta}{2\mu_{ar}} \tag{15}$$

Where, δ is the airgap. Once calculated the Couette number it's possible to know the torque coefficient.

$$C_{M1} = 10\frac{(2\delta/D_r)^{0.3}}{Co}, \quad Co < 64, \tag{16}$$

$$C_{M1} = 1.03\frac{(2\delta/D_r)^{0.3}}{Co^{0.6}}, \quad 64 < Co < 5 \times 10^2 \tag{17}$$

$$C_{M1} = 2\frac{(2\delta/D_r)^{0.3}}{Co^{0.5}}, \quad 5 \times 10^2 < Co < 10^4 \tag{18}$$

$$C_{M1} = 0.065\frac{(2\delta/D_r)^{0.3}}{Co^{0.2}}, \quad 10^4 < Co \tag{19}$$

Regarding the friction at the end surfaces of the rotor with the air, can be obtained by:

$$P_{W2} = \frac{1}{64} C_{M2} . \rho . \Omega^3 (D_r^5 - D_{ri}^5) \tag{20}$$

Where, D_{ri}^5 is the shaft diameter. In order to calculate the new torque coefficient (C_{M2}), is necessary to calculate the Reynolds number.

$$Re = \frac{\rho \Omega D_r^2}{4\mu_{ar}} \tag{21}$$

$$C_{M2} = \frac{3.87}{Re^{0.5}}, \quad Re < 3 \times 10^5 \tag{22}$$

$$C_{M2} = \frac{0.146}{Re^{0.2}}, \quad Re > 3 \times 10^5 \tag{23}$$

Once obtained all the components of the ventilation and bearing losses, it's possible to achieve the value of the mechanical losses (P_m):

$$P_m = P_b + P_{W1} + P_{W2} \tag{24}$$

3. Thermal Modelling Based on Lumped Parameters Thermal Network

In this method, the thermal model of the machine is represented by a networks formed by nodes, resistances, capacitors and heat sources. Based on the operator objective,

the network is able to describe the three necessary forms of heat transfer [1]. Different steps are required to built the thermal model. First step consists in discretising the machine or a part into different elements. Each one of these elements is presented by a node in the grid. It is interconnected with its neighbour through thermal resistors. The heat sources indicate the heat production process and they are associated to the losses of that's element. When the study takes into account transient state analysis, the thermal capacitors are added to the heat sources in order to present the variation of energy over time [14]. It is extremely important to mention that the level of discretization (number of nodes) must be well defined. Actually, a complex grid takes a lot of time in simulation; however simple grid leads to imprecise thermal analysis. Over the last few years several LPTN models of electric machines have been developed such as the model of Mellor and Turner [15].

3.1. Motivation

Some applications such as the aeronautic and nuclear context require the control online of the IM temperature with an acceptable accuracy. There are a hardware solution which consists in the inter thermal sensors with the data acquisition system. This solution is the most rapid and it provides a high precision measurements. However, it is a costly procedure. The key will be a new LPTN which presents a compromise between simplicity (small number of nodes), accuracy and rapidity.

3.2. Thermal model: LPTN model

The model used in this paper is illustrated in the figure.1. This model takes in consideration the heat transfers occurred in the machine and allows obtaining the temperature of the follow components: stator teeth (T_{th}), stator windings (T_{win}), insulation (T_{ins}), contact surface between insulation and stator core (T_{ins-co}), stator core (T_{co}), contact surface between stator core and frame(T_{co-fr}) and frame (T_{fra}). Applying the equation of heat for a hollow cylinder with the boundary respective to each case, it's possible to obtain the thermal resistances of the several components.

$$R_{th} = \frac{1}{4.\pi.l_r.\lambda_{th}} \left[1 - 2\left(\frac{r_1^2}{r_2^2 - r_1^2}\right) ln\left(\frac{r_2}{r_1}\right)\right] \tag{25}$$

$$R_{win} = \frac{1}{4.\pi.l_r.\lambda_{win}} \left[1 - 2\left(\frac{r_2^2}{r_3^2 - r_2^2}\right) ln\left(\frac{r_3}{r_2}\right)\right] \tag{26}$$

$$R_{ins} = \frac{\ln\left(\frac{r_4}{r_3}\right)}{2.\pi.l_r.\lambda_{ins}} \tag{27}$$

$$R_{ins-co} = \frac{r_5}{2.\pi.l_r.r_4} \tag{28}$$

$$R_{co} = \frac{1}{4.\pi.l_r.\lambda_{co}}\left[1 - 2\left(\frac{r_5^2}{r_6^2 - r_5^2}\right)\ln\left(\frac{r_6}{r_5}\right)\right] \tag{29}$$

$$R_{co-fra} = \frac{r_7}{2.\pi.l_r.r_6} \tag{30}$$

$$R_{fra} = \frac{ln\left(\frac{r_8}{r_7}\right)}{2.\pi.l_r.\lambda_{fr}} \tag{31}$$

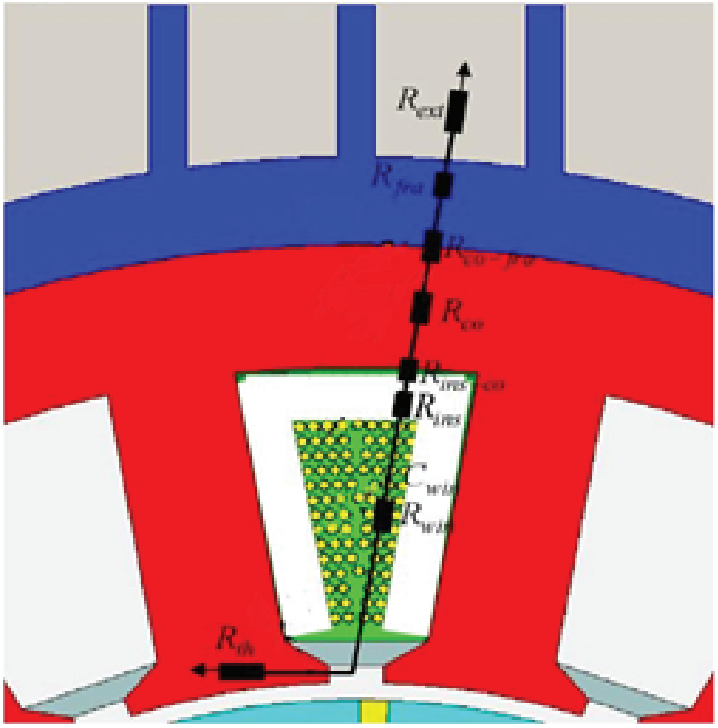

Figure 1: IM thermal model, based on the LPTN.

Once the thermal resistances are computed it becomes possible to calculate the temperatures in the steady state.

$$T_{th} = (R_{win} \times (P_f + P_m)) + T_{win} \tag{32}$$

$$T_{win} = R_{ins} \times (P_t) + T_{ins} \tag{33}$$

$$T_{ins} = R_{ins-co} \times P_t + T_{ins-sc} \tag{34}$$

Table 1: Thermal resistances

Thermal resistances	Definition	Value [K/W]
R_{ext}	Environment	0.6200
R_{fra}	Frame	0.0048
R_{co-fra}	Contact resistance: stator coreframe	1.1020e-04
R_{co}	stator core	0.1023
R_{ins-co}	Contact resistance: insulatorstator core	0.0024
R_{ins}	Insulator	0.2385
R_{win}	Windings	4.1062e-04
R_{th}	Teeth	0.1903

$$T_{ins-sc} = (R_{co} \times (P_j + P_f)) + T_{sc} \tag{35}$$

$$T_{sc} = (R_{co-fr} \times (P_j + P_f)) + T_{sc-fra} \tag{36}$$

$$T_{sc-fra} = (R_{fra} \times P_t) + T_{fra} \tag{37}$$

$$T_{fra} = (R_{ext} \times P_t) + T_{ext} \tag{38}$$

Where P_t represents the total losses occurred in the machine. The table 1 presents the differents values of the thermal resistances.

4. Simulation Results of Healthy Mode Operation

The motor under study is an IM with a rated power equal to 1.5 kW. The different parameters are shown in the table 2.

Figure. 2 and 3 shows the three phase currents in the stator and rotor. Although, the currents decrease with time and reach the steady state at 0.5s. The stator currents stabilize at about 4 A and the rotor currents at 0 A as it is expected.

The stator and rotor fluxes as the other characteristics stabilize at 0.5s. The stator flux has a magnitude slightly bigger than rotor, but both are close to the maximum 1 Wb.

Figure. 6, shows that the motor reach is maximum speed in about 0.5 s. For a two-pole machine fed by a 50 Hz frequency the synchronous speed is 3000 rpm, which is corroborated with the obtained graphic. In figure.7 it's possible to analyze the torque behavior, which stabilizes in 0 at 0.5s. The torque of the machine is zero since the resistave torque is null.

Analysing the temperatures reached by the machine, it's possible to realise that the component with higher temperature was the stator teeth and the insulation. That can

Table 2: IM parameters.

Parameters	Values
Rated power	1.5 kW
Stator resistance	3.8 Ω
Rotor resistance	4.85 Ω
Stator inductance	0.258 H
Rotor inductance	0.258 H
Mutual inductance	0.258 H
Number of pole pairs	2
Moment of inertia	0.031 kg/m^2

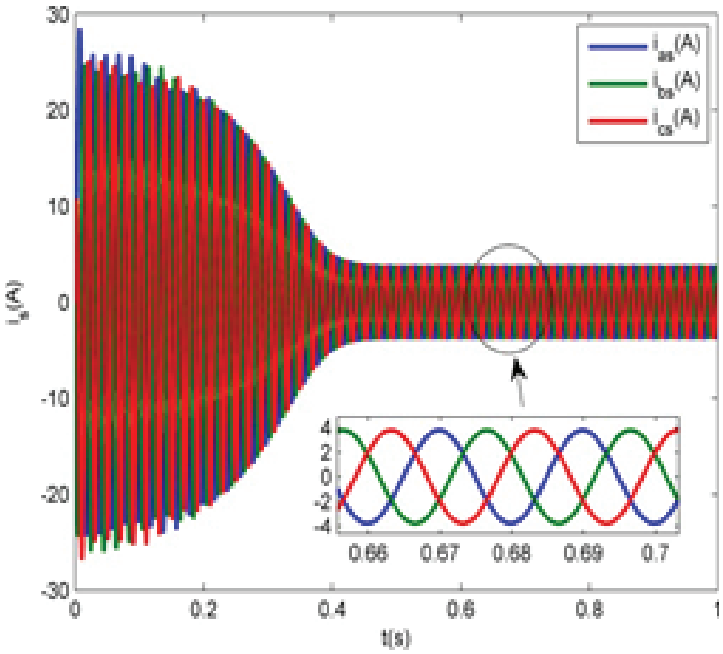

Figure 2: transient and steady state behavior of the stator current in function of time.

Table 3: Temperature results

Temperatures	Value [°C]
T_{ext}	20
T_{fr}	48.3870
T_{co-fr}	48.6068
T_{co}	34.7881
T_{ins-co}	41.2169
T_{ins}	41.3268
T_{win}	52.2466
T_{th}	52.2588

be explained by his proximity to the zones where are heat generation. The frame was

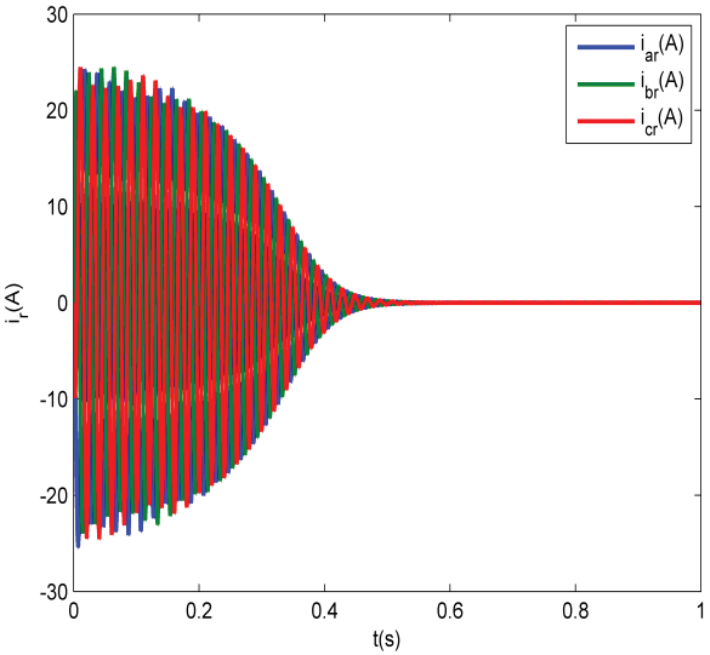

Figure 3: IM rotor current in function of time.

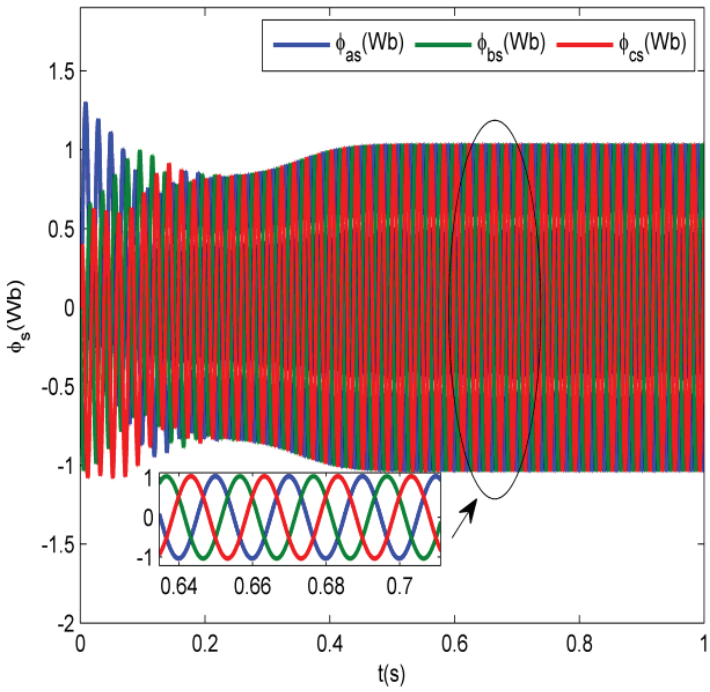

Figure 4: IM Stator flux linkage in function of time.

the component which reached the lower temperature because it is in contact with the environment.

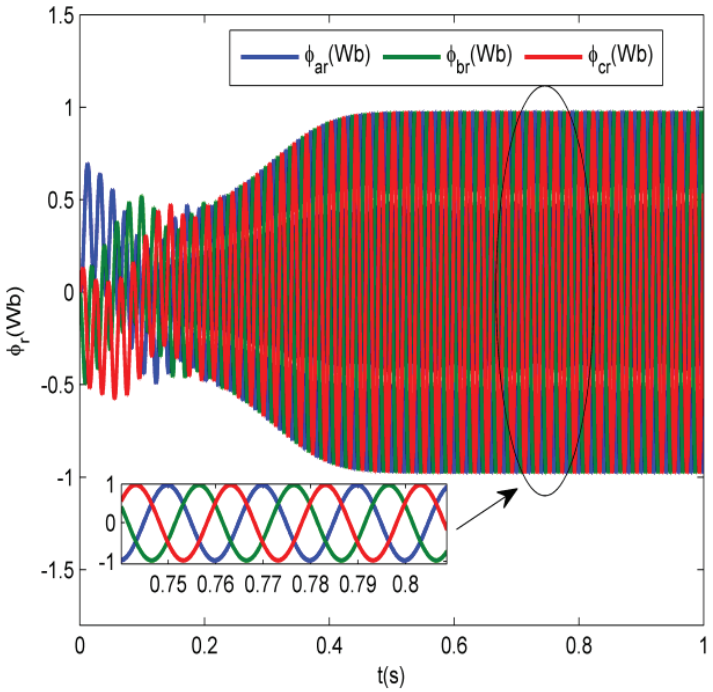

Figure 5: IM rotor flux linkage in function of time.

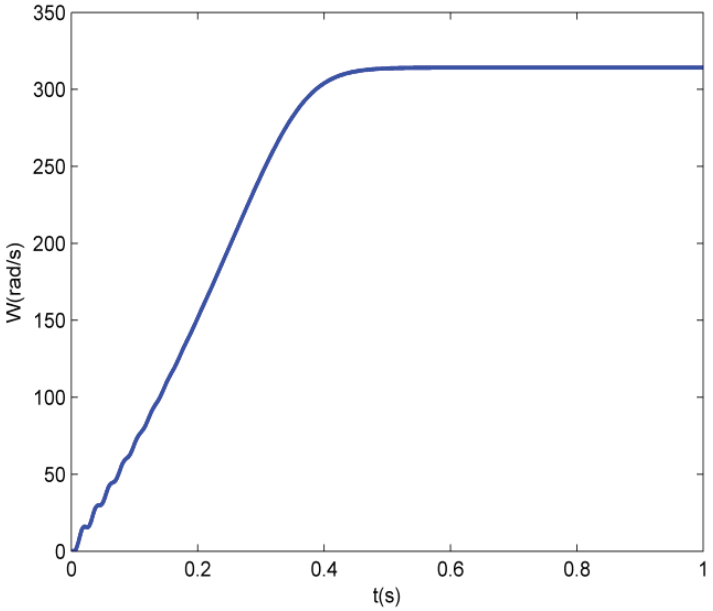

Figure 6: IM rotational speed in function of time.

5. Conclusion

In the paper, a simple thermal model of the IM has been presented. The temperatures of the machine were obtained through the application of the heat diffusion equation in a cylinder. The developed model is based on dimensional data and physical and thermal constants of the materials. The simulations results achieved are in agreement

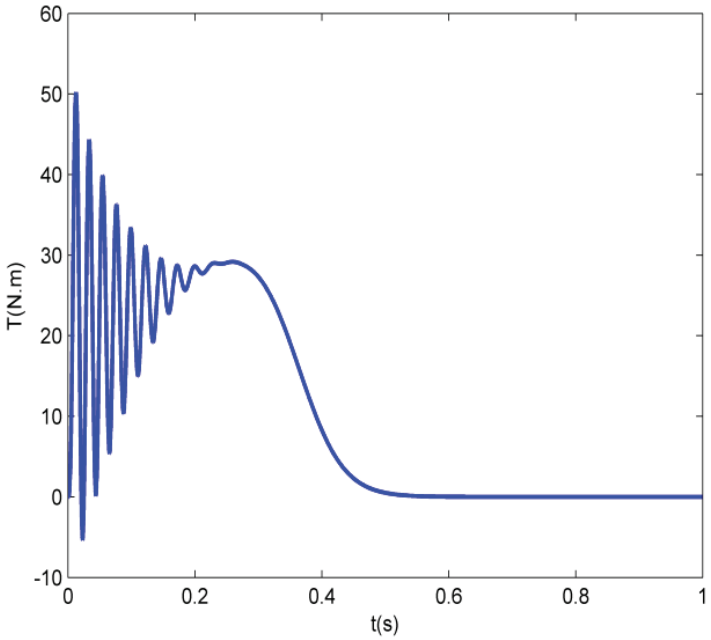

Figure 7: IM torque in function of time.

with other thermal analysis realized in similar motors. Although, for more precise results, the level of discretization of the model must be improved.

Acknowledgment

This work was supported by the European Regional Development Fund (ERDF) through the Operational Programme for Competitiveness and Internationalization (COMPETE 2020), under Project POCI-01-0145-FEDER-029494, and by National Funds through the FCT - Portuguese Foundation for Science and Technology, under Projects PTDC/EEI-EEE/29494/2017 and UID/EEA/04131/2019.

References

[1] A. Bousbaine. *An Investigation Into The Thermal Modelling of Induction*. Sheffield, England, 1993.

[2] VARIABLE SPEED DRIVES, ”lessons in efficient driving”.*Electrical Review*, pp.13-16.

[3] M. R. Feyzi. *Thermal Modelling of Deep Bar Induction Motor at Stall*. Adelaide, Australia, 1997.

[4] E. S. Hamdi. *Design of Small Electrical Machines*. John Wiley & Sons., New York, USA, 1994.

[5] Adouni, A.; Cardoso, A. J. M.: ”Thermal Analysis of Synchronous Reluctance Machines – A Review”*; Electric Power Components and Systems,”* Vol. 47, n° 6-7 (2019), pp. 471-485.

[6] Boglietti, A.; Cavagnino, A.; Staton, D. et al.: “Evolution and Modern Approaches for Thermal Analysis of Electrical Machines” *IEEE Transactions on Industrial Electronics,* Vol. 56 n° 3 (2009), pp. 871-882.

[7] Ahmed, F.; Ghosh, E.; KAR, N. C.: “Transient thermal analysis of a copper rotor induction motor using a lumped parameter temperature network model.” In *: 2016 IEEE Transportation Electrification Conference and Expo (ITEC)*, Dearborn, MI, USA, 26 – 29 June 2016. pp. 1-6.

[8] Oraee, H.: “*A quantative approach to estimate the life expectancy of motor insulation systems*,” IEEE Transactions on Dielectrics and Electrical Insulation. Vol. 7 n° 6 (2000), pp. 790-796.

[9] Bellure, A.; Aspalli, M. S.: “Dynamic d-q Model of Induction Motor Using Simulink” *International Journal of Engineering Trends and Technology*, Vol.24 n ° 5 (2015).

[10] Kylanler. G.: Thermal modelling of small cage induction motors. Gothenburg, Sweden, 1995.

[11] B. Tekgun.: Analysis, *Measurement and Estimation of the Core Losses in Electrical Machines.* Ph dissertation, University of Akron, Ohio, USA, 2016.

[12] J. Pyrhonen, T. Jokinen, V.Hrabovcová. *Design of Rotating Electrical Machines*. John Wiley & Sons, Ltd. UK, 2008.

[13] P. L. Alger. *Induction Machines*. Gordon and Breach Science Publishers, Inc. Chicago, USA, 1996.

[14] M. N. Ozisik. *Heat Transfer - A Basic Approach*. p. 1301, McGraw Hill. New York, USA, 1995

[15] D. Gerling,G.Dajaku. *Novel lumped-parameter thermal model for electrical systems*. p. 1301, Public Press, Inc. Neubiberg, Germany.